TWO-PHASE FLOW PATTERNS DURING EVAPORATION OF THE NEW REFRIGERANTS IN HORIZONTAL TUBES

by

N. Kattan, J.R. Thome* and D. Favrat

Laboratoire d'Energétique Industrielle (LENI/DME)
Ecole Polytechnique Fédérale de Lausanne
CH-1015 Lausanne, Switzerland
Telephone: (021) 6933505; Fax: (021) 6933502

ABSTRACT:

Flow pattern data for horizontal intube flow boiling are presented for refrigerants R-134a and R-402(60/2/38). The flow pattern observations were compared with various criteria for determining whether the entire circumference of a horizontal evaporator tube is wet or only partially wet, an important aspect of predicting flow boiling heat transfer coefficients. Use of only the liquid Froude number Fr_L (utilized by numerous flow boiling correlations) is shown to be too simplistic and not reliable. A new semi-empirical method of Klimenko and Fyodorov appears to be promising. The observed flow patterns were also compared to several flow pattern maps, showing limited success.

---

* Will attend and present the paper at the meeting.

Paper H2
European Two-Phase Flow Group Meeting
June 7-10, 1993, Hannover, Germany

INTRODUCTION

A comprehensive test program on two-phase flow and heat transfer to the new generation of environmentally-safe refrigerants is underway at the Laboratoire d'Energétique Industrielle (LENI). New refrigerants tested so far include R-123 [a substitute for R-11], R-134a [a substitute for R-12 and R-22] and R-402(60/2/38) [a substitute for R-502 produced by Du Pont de Nemours (tradename Suva HP80) that is a non-azeotropic ternary mixture composed of 60% R-125, 2% propane and 38% R-22 by wt.].

The present paper focuses on two-phase flow patterns for forced flow evaporation inside horizontal tubes with refrigerants R-134a and R-402(60/2/38). Results obtained so far cover a narrow range of mass velocities but a wide range of vapor qualities. The flow patterns observed are for diabatic test conditions while most flow pattern maps were developed from adiabatic test data. Flow patterns and boiling phenomena observed for evaporation of R-11 and R-123 inside horizontal annuli were reported earlier in Kattan, Thome and Favrat (1992).

For evaporation inside tubes the knowledge of the local two-phase flow pattern is very important for building a mechanistic-type of method for predicting boiling heat transfer coefficients. For horizontal flows the stratification of the liquid to the lower portion of the tube has a significant adverse affect on the heat transfer coefficient. Thus development of accurate criteria for predicting the onset of stratification and local flow patterns is an important step to improving upon the existing flow boiling correlations that are completely empirically-based.

TEST FACILITIES, MEASUREMENT SYSTEMS AND PROCEDURES

The experimental work was conducted using the new LENI test facility, built to exacting detail over the past three years with very accurate measurement and control systems. The test facility is capable of performing both single-phase and two-phase heat transfer and pressure drop tests. The first feature is used to measure single-phase heat transfer coefficients for augmented tubes, such as internally finned tubes. Two-phase experiments are utilized to obtain local boiling heat transfer coefficients, pressure drops and flow patterns. Flows can be investigated for test sections in any orientation (horizontal, vertical or inclined) although only the horizontal orientation was used here.

Figure 1 depicts a simplified flow diagram of the test facility. It has four double-pipe test sections (only two are shown). One pair of double-pipe sections mounted in series is used for evaporating the refrigerant inside the inner tube and the another pair is used for evaporating the refrigerant flowing in the annulus. Hot water can be directed to either pair of test sections for heating under countercurrent flow conditions.

As shown in Figure 1, the refrigerant passes through two preheaters before reaching the first test section. A manually-controlled expansion valve is located before the first test section to regulate the inlet vapor quality. After the

refrigerant is partially evaporated in the two test sections, it enters a coiled tube-in-tube condenser where the refrigerant is condensed and subcooled. Next the refrigerant is drawn into a stainless steel pump with a magnetically driven rotor, the latter which operates without any lubricating oil and eliminates any possibility of oil entering the refrigerant circuit. A precision bypass valve around the pump is used to modify the refrigerant flow rate. The refrigerant passes through a calibrated Coriolis flow meter and back into the preheaters.

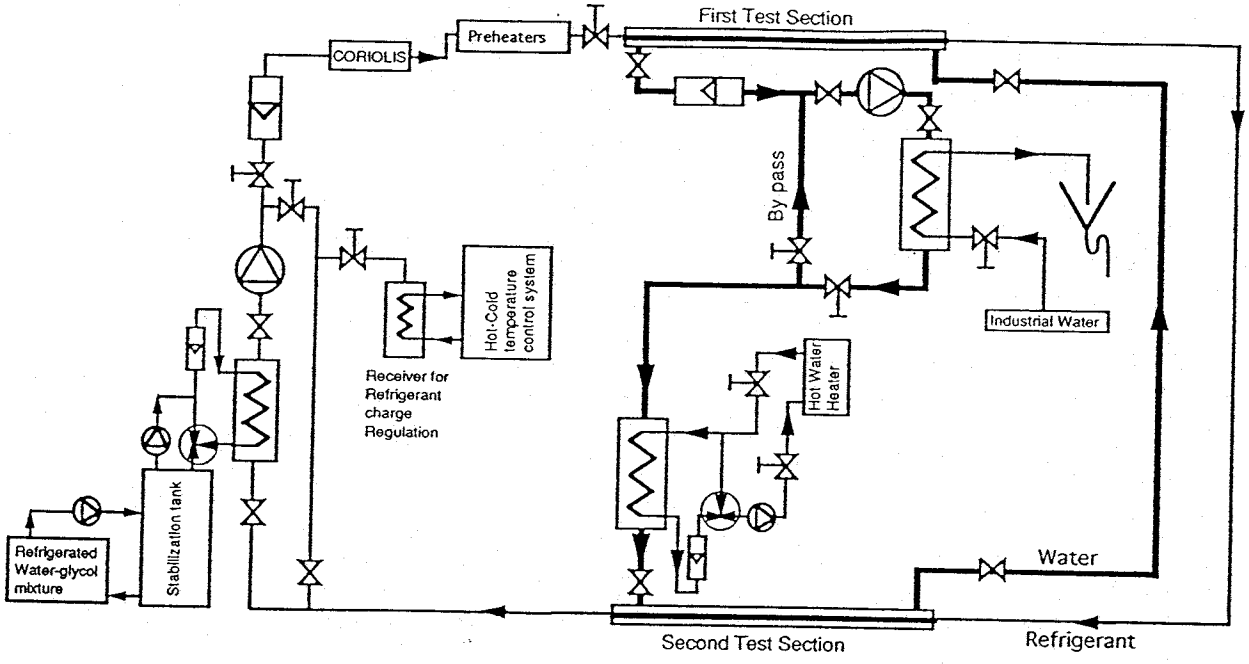

Figure 1. Layout of test facility flow circuits.

A temperature-controlled receiver is connected via a valve to the refrigerant circuit to regulate the amount of refrigerant charge. A vacuum pump system (not shown) can be connected for evacuation of the circuit when changing over from one refrigerant to another and for leak detection. After charging, the refrigerant is vigorously boiled for several hours and noncondensable gases (if any) are removed via a bleed valve. For R-402(60/2/38), no bleeding is performed since this could change the composition of the mixture.

The hot water heater circuit reheats the water after it passes through the two test sections. High purity, distilled water is utilized to avoid fouling; visual inspection of the tubes confirms that none occurs. The water flow rate is measured by a calibrated, high quality float meter. The water is circulated by a stainless steel pump similar to the refrigerant circuit's to eliminate any possibility of lubricating oil entering the water circuit and thus affecting the energy balances. This system is also carefully deaerated to eliminate any adverse effects on flow rate measurements and energy balances.

The refrigerated water-glycol solution for the system's coiled tube-in-tube condenser is maintained at a fixed inlet temperature by a refrigeration system with a large water-glycol receiver in the flow circuit. This setup eliminates cyclic temperature variations in the condenser and thus in the test

refrigerant circuit that can be caused by the refrigeration system's on-off operating cycle when no receiver is used.

The inside tubes of the double-pipe test sections are made with plain copper tubes for the present tests. They are 12.00 mm internal diameter, 14.00 mm outside diameter and 3.20 m long. The outside tubes are a novel design; they are precision machined in two halves from PVC Hard, which is a very tough and durable plastic material that also acts to insulate the test section. This allows the dimensions to be very precise and uniform along the length, much more than standard piping used in other experimental test facilities. An O-ring is compressed between the two halves to form the seal such that the faces of the two halves meet to form a circular annulus around the copper tube. The internal diameters of the PVC tubes are 19.00 mm such that the gaps in the annuli are 2.50 mm. O-ring sealed screws are inserted through the PVC to center the copper tubes inside. The PVC tubes are supported to maintain perfectly straight test sections. The two test sections are each 3.013 m long for heat transfer measurement purposes.

Tubular sight glasses about 75 mm long with an internal diameter of 12.00 mm are installed inline with the copper tubes to visualize the flow patterns at the four inlet and outlet locations. A high speed Sony video tape camera running at up to 10,000 frames/sec is used to record the flow patterns. The tapes are then viewed to identify the specific type of flow pattern for the test conditions as a function of mass velocity, vapor quality, and saturation temperature and pressure for the particular refrigerant.

Figure 2 shows the measurement layout diagram for water flowing in the annuli and refrigerant flowing counter-currently inside the inner tubes. At the refrigerant inlet, the temperature is measured by thermocouple #600 located in the refrigerant flow stream (the tube is well insulated from this point up to the location of the four water-side thermocouples #614, #613, #501 and #615 with a tightly-fitted teflon sleeve). Similar arrangements exist for the refrigerant at the outlet of the first test section, the inlet to the bottom test section and the exit of the bottom test section, temperatures #601, #602 and #603, respectively. At each of these locations the absolute pressures of the refrigerant and the differential pressure drops across the two test sections are measured.

On the water-side, four thermocouples are installed at each measurement location in the annulus at 0°, 60°, 120° and 180° from the top of the annulus. These are inserted through sealed screws installed in the thick PVC tube wall with the junctions positioned about 1 mm from the copper tube wall. There are four measurement locations on both the top and bottom test sections; thus, there are six test zones to obtain heat transfer coefficients over narrow changes of vapor quality (essentially local values) during boiling or condensation tests. This novel approach eliminates inlet, outlet and "dead" zones formed at the connections to the mixing chambers used in conventional setups that alter the local water-side heat transfer coefficients over a significant percentage of the test section length. Using our setup, a minimum of flow disruption of the water flow results (only four small diameter thermocouple elements); the highly accurate energy balances confirm the accuracy of this approach.

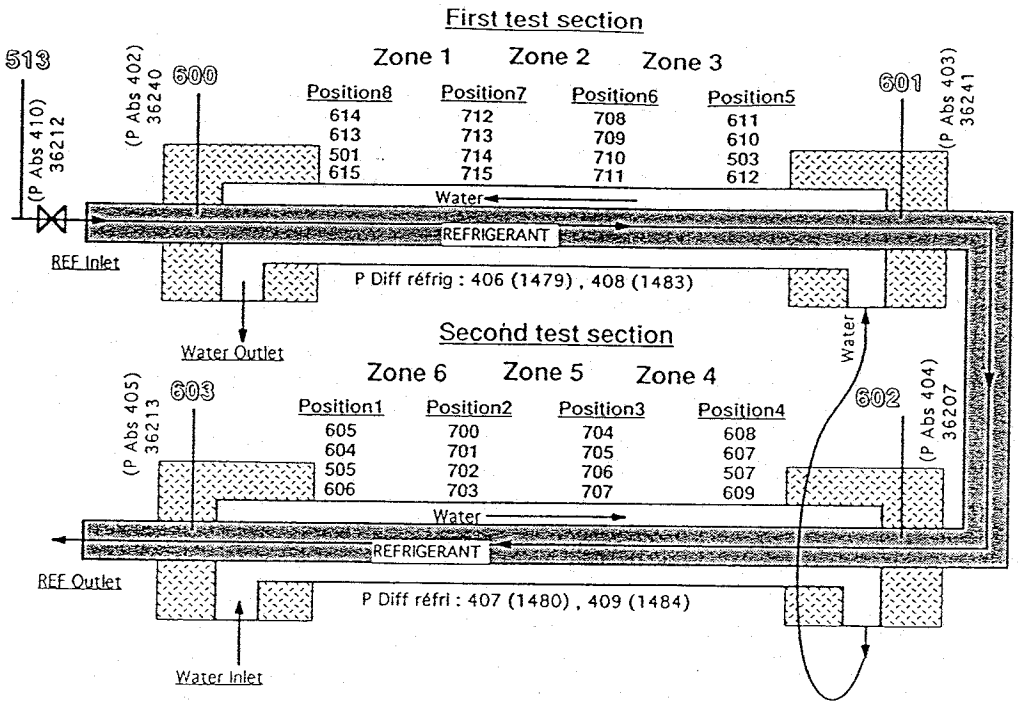

Figure 2. Measurement locations in the test sections.

An HP 3852A data acquisition system together with a Macintosh IIX personal computer running the LabView software are used to acquire, analyze and store the data. All sensors are carefully calibrated. The thermocouples are calibrated using the double precision method available in the acquisition system to obtain the highest accuracies possible, that is 0.03°C. For adiabatic conditions after leaving the rig off all night, all temperatures are within a maximum deviation of 0.10°C and most are within 0.05°C of the average. For diabatic test conditions, the maximum variations between the four thermocouple readings around the annuli at any one position are normally within 0.10°C or less for $Re_D > 4000$ while slightly larger (0.20-0.30°C) for $Re_D < 4000$, where thermal stratification begins to be significant due to the natural convection effects of mixed convection. The uniformity of these temperature measurements also confirms the precision centering of the copper tube.

The computerized control system maintains the system at steady-state during tests and then is used to bring the system to the next test condition. Data acquisitions of the test variables show that no fluctuations or cyclic changes in temperatures, pressures or flow rates occur during tests. Subroutines calculate test variables in order to run the experiments at specific conditions.

The refrigerant flow rate is measured with an estimated accuracy of 0.2% and the water flow rate to within 1.0%, based on our calibrations. The energy balances between the water and refrigerant flows in the two test sections agree to within 2% maximum error (1% average error) when the water Reynolds number is maintained above 4000, which is within the accuracy of published specific heat values for refrigerant and water. Errors can rise to 3-5% or more for $Re_D < 4000$ because of the thermal stratification effect and hence this regime is avoided.

TEST FLUIDS

Intube evaporation tests were run with pure refrigerant R-134a and the ternary non-azeotropic blend R-402(60/2/38). So far tests with videos of R-134a have only been run at one mass velocity (100 kg/m^2 s) and at one saturation condition (10.7°C and 4.246 bar). Table 1 shows the physical properties of R-134a at this saturation temperature determined from the methods presented in Thome (1993). Tests with R-402(60/2/38) have been run so far at a bubble point temperature of 1.92°C (7.05 bar) for mass velocities of 102 and 200 kg/m^2 s. Table 2 depicts the mixture physical properties at this test condition, where the thermodynamic properties were obtained from Du Pont (1993) and the transport properties from REFPROP (1992).

Table 1. R-134a Thermophysical Properties.

Saturation Temperature (°C)	10.7
Saturation Pressure (bar)	4.246
Liquid Density (kg/m^3)	1256.5
Vapor Density (kg/m^3)	20.73
Liquid Dynamic Viscosity (cp)	0.2458
Vapor Dynamic Viscosity (cp)	0.0115
Liquid Specific Heat (kJ/kg K)	1.3736
Vapor Specific Heat (kJ/kg K)	0.9347
Liquid Thermal Conductivity (W/m K)	0.0896
Vapor Thermal Conductivity (W/m K)	0.0131
Surface Tension (N/m)	0.0102
Latent Heat of Vaporization (kJ/kg)	190.0
Critical Pressure (bar)	40.56
Critical Temperature (K)	374.21
Molecular Weight	102.03

Table 2. R-402(60/2/38) Thermophysical Properties.

Saturation Temperature (°C)	1.92
Saturation Pressure (bar)	7.05
Liquid Density (kg/m^3)	1263.4
Vapor Density (kg/m^3)	34.79
Liquid Dynamic Viscosity (cp)	0.2052
Vapor Dynamic Viscosity (cp)	0.0122
Liquid Specific Heat (kJ/kg K)	1.280
Vapor Specific Heat (kJ/kg K)	0.675
Liquid Thermal Conductivity (W/m K)	0.0654
Vapor Thermal Conductivity (W/m K)	0.0106
Surface Tension (N/m)	0.0892
Latent Heat of Vaporization (kJ/kg)	159.7
Critical Pressure (bar)	41.35
Critical Temperature (K)	348.65
Molecular Weight	101.55

TWO-PHASE FLOW PATTERNS

Figure 3 taken from Collier and Thome (1993) depicts the two-phase flow patterns that may be observed along a horizontal evaporator tube. Depending on the flow conditions, not all of these patterns may occur or be seen at one time.

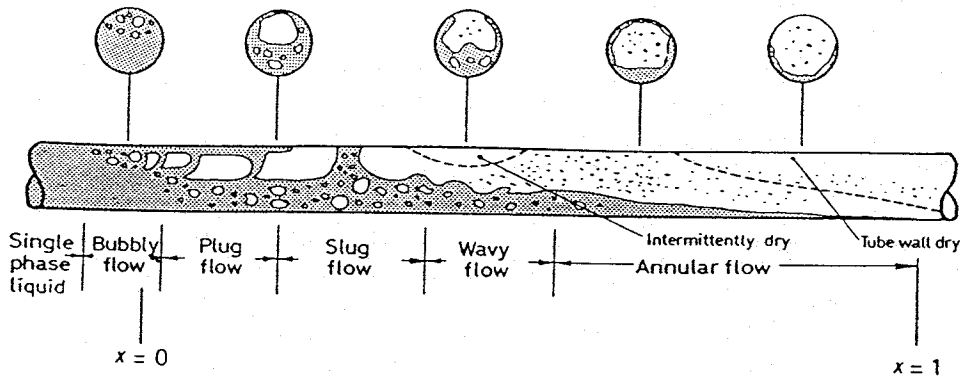

Figure 3. Flow patterns for evaporation in a horizontal tube.

The flow patterns observed in the high speed video tapes (2000 frames/sec) at the exit of the two test sections were classified according to the following definitions:

S - Stratified flow: Liquid and vapor phases flow separately, the liquid below and the vapor above a relatively smooth horizontal interface.

SW - Stratified wavy flow: Liquid and vapor phases flow separately one below the other, respectively, with waves disrupting the interface (the waves however do not reach the top of the tube). Entrainment of droplets in the vapor phase can occur.

I - Intermittent flow: The fluid flows as liquid slugs separated by vapor zones containing a stratified wavy liquid layer flowing in the bottom of the tube. Entrained vapor bubbles are in the slugs concentrated near the top of the tube. The upper part of the tube remains wet from the residual liquid film left behind by the slug.

A - Annular flow: Liquid and vapor phases flow separately with the liquid on the tube wall and the vapor in the central core. The liquid film is much thicker at the bottom of the tube than at the top. The upper part or even the majority of the tube wall may be dry as depicted at the right end of Figure 3. (For a thin, very chaotic liquid film covering only the bottom fraction of the tube, it is difficult to differentiate between annular flow with partial dryout and stratified wavy flow). Entrainment of liquid droplets can occur from the very disrupted interface.

MF - Mist flow: The vapor phase is the only continuous phase and liquid is present in the form of droplets (these atomized droplets are sometimes too small to see).

For intube evaporation, it is important to know whether or not the entire tube wall is continuously wetted with liquid at local conditions along the tube. For locations where there are dry spots, the heat transfer process between the vapor and tube wall is only single-phase forced convection with values significantly below those for nucleate boiling, convective boiling or film evaporation. The video tapes were also viewed to determine whether the tube wall was wetted all around the circumference or only partially wetted. It was not always possible to be completely sure.

TWO-PHASE FLOW PATTERN TEST RESULTS

The flow pattern data for R-134a are shown in Table 3 with the test conditions cited. The flow pattern data for R-402(60/2/38) are depicted in Tables 4 and 5 for two mass velocities. The liquid Froude numbers are shown and also the Klimenko and Fyodorov factor defined later in Eq. (2). More tests over a wider range of mass velocities are now underway.

Table 3. Flow Patterns Observed for R-134a at Mass Velocity of 100 kg/m^2 s.

Test # *	Mass Velocity (kg/m^{2}s)	Local Vapor Quality	Flow Pattern Observed	Notes	Wetting (All or Partial)	Fr_L Froude Number	K&F Factor Eq.(2)
1T	94.3	0.198	S/SW	(3)	Partial	0.048	0.076
2T	101.7	0.161	I/SW	(3)	Partial	0.056	0.204
2B	"	0.327	SW	(1)	Partial?	"	0.175
3T	98.9	0.180	I/SW	(3)	Partial	0.053	0.076
4T	103.9	0.199	SW	(1)	Partial?	0.058	0.093
5T	100.9	0.225	SW	(1)	Partial?	0.055	0.101
6T	104.2	0.257	SW	(1)	Partial?	0.058	0.129
6B	"	0.653	A	(2)	Partial	"	0.644
7B	104.8	0.716	A	(2)	Partial	0.059	0.778
8B	95.8	0.872	A	(2)	Partial	0.049	0.961
9T	103.3	0.342	SW	(1)	Partial?	0.057	0.194
9B	"	0.848	A	(2)	Partial	"	1.056
10T	98.9	0.373	SW	(1)	Partial?	0.053	0.206
10B	"	0.844	MF		All Dry	"	0.959
11T	95.0	0.413	SW	(1)	Partial?	0.049	0.227
11B	"	0.924	MF		All Dry	"	1.060
12T	103.5	0.507	SW	(1)	Partial?	0.058	0.391

* T - End of top test section, B - End of bottom test section;
? Thin liquid film on top portion of tube may or may not be always present;
(1) Close to Annular with some intermittent liquid film on top portion of tube;
(2) Tube wall is partially dry with liquid only in lower 1/4 of tube or less;
(3) Near transition from 1st regime to 2nd regime.

Table 4. Flow Patterns Observed for R-402(60/2/38) at Mass Velocity of 102 kg/m^2 s.

Test # *	Mass Velocity (kg/m^{2}s)	Local Vapor Quality	Flow Pattern Observed	Notes	Wetting (All or Partial)	Fr_L Froude Number	K&F Factor Eq.(2)
1T	104.2	0.205	SW		Partial	0.060	0.451
1B	"	0.360	SW	(1)	Partial?	"	0.072
2T	103.0	0.229	SW		Partial	0.059	0.047
2B	"	0.445	SW	(1)	Partial?	"	0.097
3T	102.0	0.223	SW		Partial	0.058	0.046
3B	"	0.478	SW	(1)	Partial?	"	0.103
4T	102.5	0.266	SW		Partial	0.058	0.051
4B	"	0.561	A	(2)	Partial	"	0.135
5T	101.3	0.291	SW		Partial	0.057	0.054
5B	"	0.611	A	(2)	Partial	"	0.153
6T	99.7	0.317	SW		Partial	0.055	0.057
6B	"	0.690	A	(2)	Partial	"	0.185
7T	98.9	0.344	SW		Partial	0.054	0.061
7B	"	0.769	A	(2)	Partial	"	0.224
8T	99.7	0.375	SW		Partial	0.055	0.069
9T	99.7	0.444	SW		Partial	0.055	0.088
10T	103.6	0.465	SW		Partial	0.059	0.101
11T	104.1	0.527	SW		Partial	0.060	0.125
12T	101.3	0.659	SW	(1)	Partial?	0.057	0.176
13T	101.5	0.688	SW	(1)	Partial?	0.057	0.191
14T	102.2	0.743	SW	(1)	Partial	0.058	0.224
15T	101.8	0.900	I/SW	(3)	Partial	0.057	0.322

* T - End of top test section, B - End of bottom test section;
? Thin liquid film on top portion of tube may or may not be always present;
(1) Close to Annular with some intermittent liquid film on top portion of tube;
(2) Tube wall is partially dry with liquid only in lower 1/4 of tube or less;
(3) Near transition from 1st regime to 2nd regime.

Table 5. Flow Patterns Observed for R-402(60/2/38) at Mass Velocity of 200 kg/m^2 s.

Test # *	Mass Velocity (kg/m^{2}s)	Local Vapor Quality	Flow Pattern Observed	Notes	Wetting (All or Partial)	Fr_L Froude Number	K&F Factor Eq.(2)
1T	197.6	0.139	SW		Partial	0.22	0.145
1B	"	0.246	SW	(1)	Partial?	0.22	0.180
2T	200.5	0.162	I		All Wet	0.22	0.154
2B	"	0.294	SW	(1)	Partial?	0.22	0.213
3T	199.0	0.168	I		All Wet	0.22	0.153
3B	"	0.320	SW	(1)	Partial?	0.22	0.229
4T	199.9	0.174	I/SW	(3)	Partial	0.22	0.156
4B	"	0.332	SW	(1)	Partial?	0.22	0.241
5T	201.3	0.178	I/SW	(3)	Partial	0.22	0.159
5B	"	0.353	SW	(1)	Partial?	0.22	0.261
6T	199.7	0.196	I/SW	(3)	Partial	0.22	0.162
6B	"	0.391	SW	(1)	Partial?	0.22	0.293
7T	199.0	0.201	I/SW	(3)	Partial	0.22	0.163
7B	"	0.420	A	(2)	Partial	0.22	0.321
8T	201.9	0.220	I/SW	(3)	Partial	0.23	0.175
8B	"	0.463	A	(2)	Partial	0.23	0.382
9T	199.1	0.221	I/SW	(3)	Partial	0.22	0.171
9B	"	0.501	A	(4)	All Wet	0.22	0.421
10T	198.7	0.241	I/SW	(3)	Partial	0.22	0.179
10B	"	0.542	A	(4)	All Wet	0.22	0.477
11T	200.2	0.253	I/SW	(3)	Partial	0.22	0.188
11B	"	0.581	A	(4)	All Wet	0.22	0.547
12T	200.2	0.266	I/SW	(3)	Partial	0.22	0.195
12B	"	0.633	A	(4)	All Wet	0.22	0.637
13T	198.5	0.291	I/SW	(3)	Partial	0.22	0.207
13B	"	0.700	A	(4)	All Wet	0.22	0.755
14T	199.9	0.310	SW		Partial	0.22	0.224
14B	"	0.752	A	(4)	All Wet	0.22	0.876
15T	198.6	0.321	SW		Partial	0.22	0.229
15B	"	0.800	MF		All Dry	0.22	0.972
16T	200.1	0.336	SW		Partial	0.22	0.244
16B	"	0.816	MF		All Dry	0.22	1.026
17T	197.8	0.367	SW		Partial	0.22	0.265
17B	"	0.871	MF		All Dry	0.22	1.141
18T	198.9	0.401	SW		Partial	0.22	0.301
18B	"	0.893	MF		All Dry	0.22	1.210
19T	198.6	0.494	SW/A		Partial	0.22	0.410
19B	"	0.912	MF		All Dry	0.22	1.258
20T	202.3	0.526	SW/A		Partial	0.23	0.471
20B	"	0.918	MF		All Dry	0.23	1.323

* T - End of top test section, B - End of bottom test section;
? Thin liquid film on top portion of tube may or may not be always present;
(1) Close to Annular with some intermittent liquid film on top portion of tube;
(2) Tube wall is partially dry with liquid only in lower 1/4 of tube or less;
(3) Near transition from 1st regime to 2nd regime;
(4) Annular flow with thick liquid film at very bottom of tube and very thin liquid film over rest of tube.

Figure 4 depicts digitalized images of several flow regimes taken from the video tapes. In Figure 4(a) the image shows the stratified flow pattern for condition 1T in Table 3 for R-134a. The flow here also had occasional waves (not shown in this particular image) and thus the flow was defined to be near the transition for stratified to stratified wavy flow (S/SW). Figure 4(b) shows R-402(60/2/38) flowing through the sight glass at the end of the top evaporation test section in the stratified wavy (SW) flow pattern at condition 3T in Table 4.

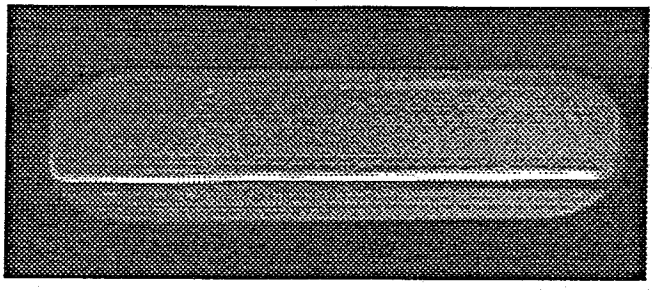

(a) Stratified flow of R-134a

(b) Stratified wavy flow of R-402(60/2/38)

Figure 4. Several flow patterns observed for the test fluids.

STRATIFICATION CRITERIA USED IN FLOW BOILING CORRELATIONS

Shah (1982), Gungor and Winterton (1986, 1987) and Kandlikar (1990) have used a very simple criterion to determine if the wall of a horizontal evaporator tube is wet. According to Shah the tube wall is only partially wetted around its circumference if the liquid Froude number $Fr_L < 0.04$, defined as

$$Fr_L = G^2/[\rho_L^2 \; g \; D] \qquad (1)$$

where G is the total mass velocity, g is the acceleration due to gravity and D is the internal tube diameter. This effect is important because the heat transfer coefficient is lower than that for a vertical tube for identical local conditions if the tube wall is partially dry.

Kandlikar evaluated his boiling databank for different values of Fr_L and retained Shah's value of 0.04. Gungor and Winterton did the same and arrived at the criterion $Fr_L < 0.05$. Thus, these criteria were derived from statistical analysis of boiling heat transfer databanks to improve correlation accuracy rather than from actual physical observations of the flows.

Examining Tables 3-5, Fr_L is always larger than 0.04 for the present data and nearly always larger than 0.05. In Tables 3 and 4, the values of Fr_L are close to the above values of 0.04 and 0.05; all flows were observed to have partially wetted walls, except those marked with a ? sign [where we were not able to establish whether the wall was continuously wet or not]. Hence the above criteria are nearly always wrong, although not by much, with partial wetting for Fr_L from 0.048 to 0.060. Instead Table 5 shows that for Fr_L from 0.22-0.23 the tube wall can be (i) partially wet, (ii) all wet or (iii) all dry while the above criteria would predict them to always be all wet. Thus, the liquid Froude number is not very safisfactory for establishing whether or not the tube wall is all wet or partially wet. In part this is because no account is made of the local vapor quality or void fraction; for a given flow rate the above criteria are applied without modification from the inlet to the outlet of an evaporator tube, which is not reasonable based on Figure 3.

Klimenko and Fyodorov (1990) have developed a mechanistic criterion for determining the transition from stratified to unstratified flow. They define unstratified flow as all flow regimes with continuous wetting of the whole tube circumference (which includes intermittent or slug flows); completely stratified flow and wavy flow (since part of the tube wall is not wetted) and annular flows with dryout over the top portion of the tube are classified as stratified flow. According to their model, transition from stratified wavy flow to annular flow is due to entrainment-deposition of liquid droplets on the tube wall while transition from stratified flow to intermittent flow depends on the development of gravitational waves on the liquid-vapor interface. Using a <u>diabatic</u> experimental boiling databank composed of both visual data and some nonvisual data (flow regime based on an intuitive analysis of boiling data with circumferential temperature measurements around the tube wall), they determine the constants and exponents for their following semi-empirical expression:

$$F = 0.074\ Fr_L\ (D/b)^{0.67}\ Fr_V + 8\ [1 - (\rho_V/\rho_L)^{0.1}]^2\ Fr_L \qquad (2)$$

where: $F > 1.0$ Unstratified flow exists
$F < 1.0$ Stratified flow exists

They defined the liquid Froude number using the superficial liquid velocity (u_L) such that

$$Fr_L = \rho_L\ u_L^2\ /[(\rho_L - \rho_V)\ g\ D] \qquad (3)$$

and the vapor Froude number using the superficial vapor velocity (u_V):

$$Fr_V = \rho_V\ u_V^2\ /[(\rho_L - \rho_V)\ g\ D] \qquad (4)$$

The tube internal diameter is D, g is the acceleration due to gravity (9.81 m/s^2) while b is the Laplace constant given as:

$$b = \{\sigma_L/[g\ (\rho_L - \rho_V)]\}^{1/2} \qquad (5)$$

The liquid and vapor superficial velocities are determined from the following expressions where x is the vapor quality and G is the total mass flux:

$$u_L = G\ (1-x)/\rho_L \quad (6)$$

$$u_V = G\ x/\rho_V \quad (7)$$

Examining Table 3, the last column lists values of F as the "K&V Factor". Only two values are above 1.0 (one partially wet and one all dry) which do not agree with the above criterion. However, the other flow observations agree with this criterion, neglecting those for which this condition could not be established (those with the ? sign). The flow observations in Table 4 also agree with the above criterion of Klimenko and Fyodorov. In Table 5, the agreement between the data and the stratified/unstratified flow criterion is not as good, with various "All Wet" data points having a value of F below 1.0. It should be noted that the observations marked with (4) in Table 5 have very thin liquid films along the top of the tube and are close to the dryout point. Figure 5 shows a comparison of the observations in Tables 3-5 to the Klimenko and Fyodorov criterion. On this log-log chart the agreement appears to be generally reasonable. One drawback of this method is that it does not include the transition to the mist flow regime, which is important for the accurate prediction of heat transfer coefficients at high vapor qualities in refrigeration system evaporator tubes.

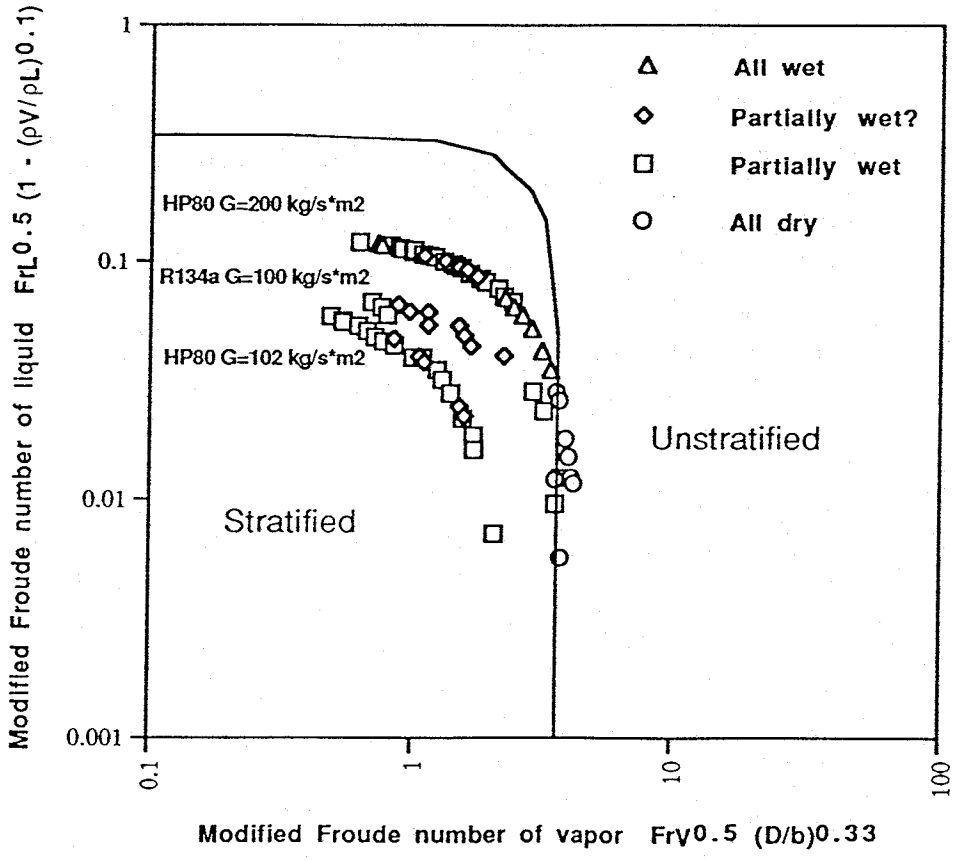

Figure 5. All data points shown on Klimenko and Fyodorov flow pattern map representing Eq. (2).

COMPARISONS TO FLOW PATTERN MAPS

A new comprehensive review of flow pattern and dryout prediction methods for vertical and horizontal flows will be available shortly in Collier and Thome (1993). The present flow

pattern observations are compared below to two flow maps.

Taitel and Dukler (1976). This is a well-known flow pattern map for adiabatic flows in horizontal tubes. It is a theoretically-based model that was originally compared to water-air data. They defined parameters F, T and K to determine the type of flow regime as a function of the Martinelli parameter X. Figure 6 shows the R-134a data at a mass velocity of 100 kg/m^2 s plotted on the Taitel-Dukler flow pattern map (with K divided by 1000). The mist flow (MF) data (not identifiable in the Taitel-Dukler map) appear in the annular flow region while the annular flow data appropriately fall in the correct region. The stratified wavy (SW) data lie just above the transition line from wavy to annular flow. The flow patterns observed to be near or at the intermittent to stratified wavy transition (I/SW) are located quite near this boundary. Instead the stratified to stratified wavy transition data point (S/SW) [stratified flow with only an occasional wavy] is considerably above its predicted boundary.

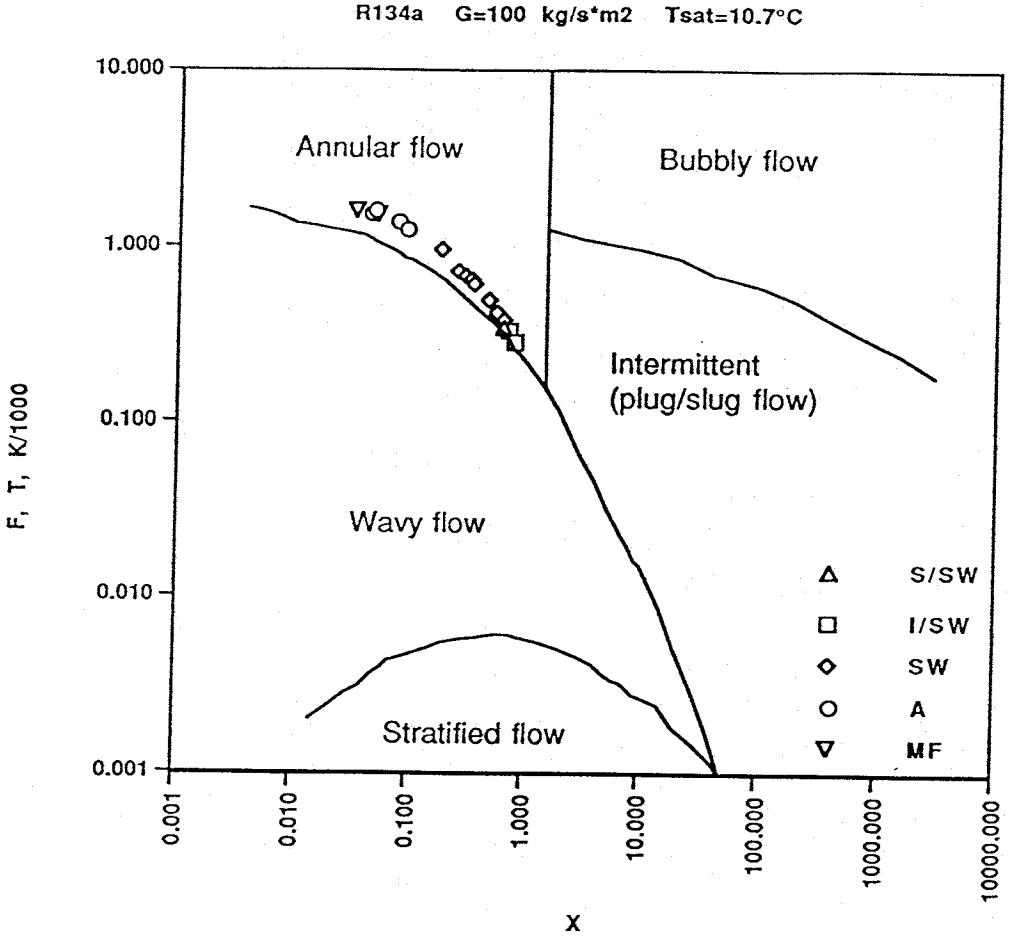

Figure 6. R-134a data plotted on Taitel-Dukler map.

The flow pattern observations for R-402(60/2/38) are plotted in Figure 7 for data at two mass velocities. Here the annular flow data are correctly located by the map while the stratified wavy flow data are just above the boundary to this regime. Most of the data for flow patterns observed to be near or at the intermittent to stratified wavy transition (I/SW) are located near this boundary.

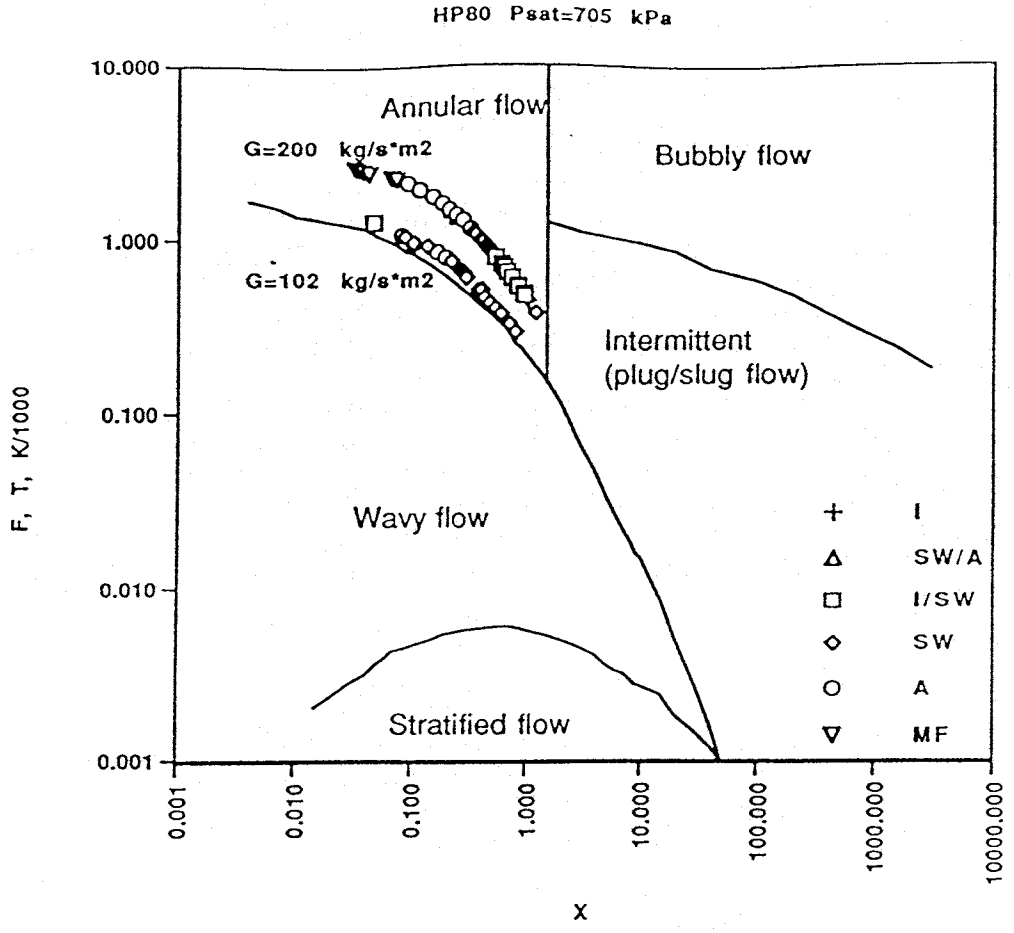

Figure 7. R-402(60/2/38) plotted on Taitel-Dukler map.

Hashizume (1983). He developed a modified Baker flow pattern map based on adiabatic horizontal flows of R-12 and R-22 inside a 10 mm bore glass tube for saturation pressures ranging from 5.7 to 19.6 bar. The Baker X parameter was redefined as

$$X = [(1-x)/x]\ \lambda\ \phi' \tag{8}$$

where the parameter λ remains the same:

$$\lambda = [(\rho_V/\rho_a)(\rho_L/\rho_{wa})]^{1/2} \tag{9}$$

The parameter ϕ' has been modified to add an exponent of 1/4 to the surface tension ratio as:

$$\phi' = (\sigma_{wa}/\sigma_L)^{1/4}\ [(\mu_L/\mu_{wa})(\rho_{wa}/\rho_L)^2]^{1/3} \tag{10}$$

The parameter Y remains the same as in the Baker flow map:

$$Y = G\ x/\lambda \tag{11}$$

Figure 8 depicts the R-134a data plotted on the Hashizume flow pattern map. The mist flow data appear in the wavy flow region while the annular flow data incorrectly fall in the stratified wavy flow region. The stratified wavy data fall in both the stratified wavy flow and the stratified flow region. The data for transition from intermittent (slug) flow to stratified wavy flow (I/SW) lie far to the left of that boundary. The data point for transition from stratified to stratified wavy flow (S/SW) is just below the indicated boundary.

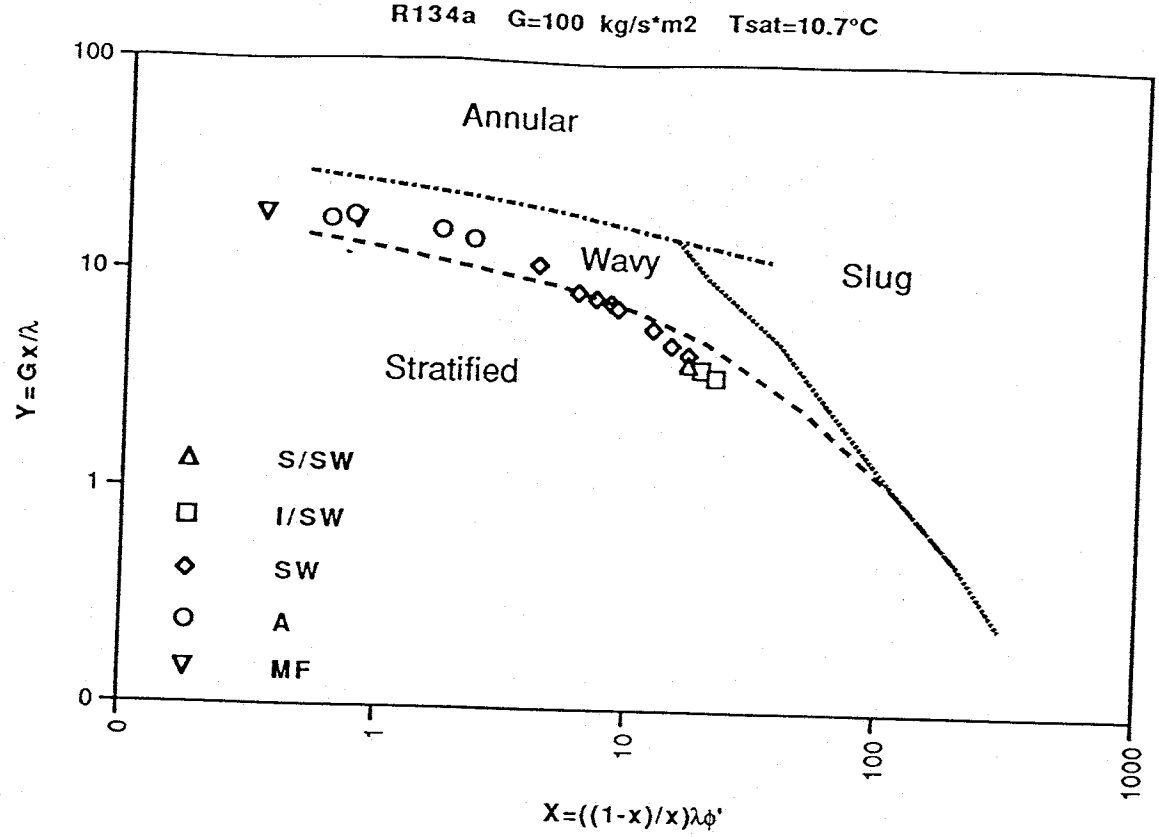

Figure 8. R-134a data plotted on Hashizume flow pattern map.

The R-402(60/2/38) flow pattern data at two mass velocities are plotted on the Hashizume map in Figure 9. Agreement between the data and the flow pattern map is not very good. The annular flow data all lie below their appropriate region while many of the stratified wavy data fall in the stratified flow region. The I/SW data are also far to the left of the predicted boundary.

CONCLUSIONS

Flow pattern data for intube flow boiling are presented for refrigerants R-134a and R-402(60/2/38). The flow patterns observed were compared with various criteria for determining whether the entire circumference of a horizontal evaporator tube is wet or only partially wet. The Shah approach using only the liquid Froude number Fr_L (defined using the total mass velocity G) is shown to be too simplistic and not reliable. The Taitel-Dukler and Hashizume flow pattern maps do not describe these limited sets of data all that well. The Klimenko-Fyodorov method appears to be the best of the four tested here. Further improvements are still required and a method that includes the transition to mist flow is required.

ACKNOWLEDGEMENTS

The research was supported by the Swiss Federal Office of Energy (OFEN), Bern. The refrigerants were provided by DuPont de Nemours International S.A. of Geneva. The authors would like to thank K. Widmer and A. Bayini for their contributions.

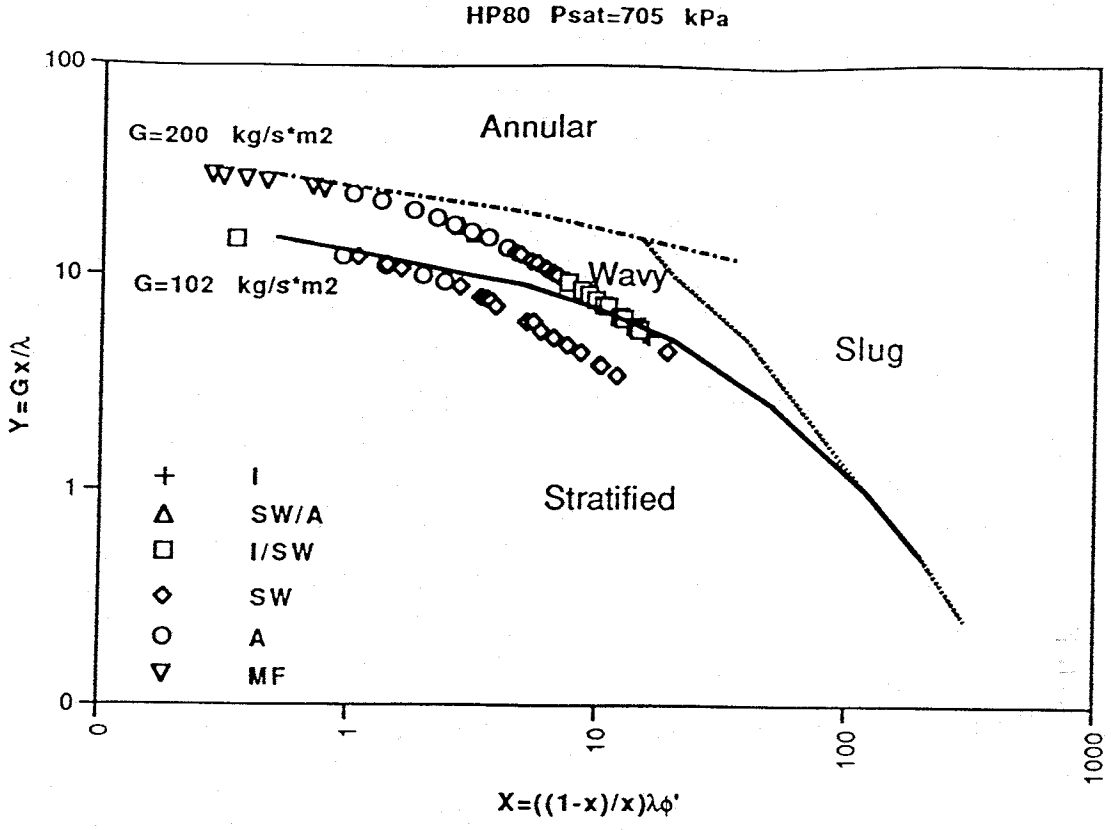

Figure 9. R-402(60/2/38) plotted on Hashizume flow pattern map.

NOTATION

b	Laplace constant
D	Tube diameter (m)
F	Factor in Eq. (2)
F	Taitel-Dukler parameter
Fr_L	Liquid Froude number
Fr_V	Vapor Froude number
G	Total mass velocity (kg/m^2 s)
g	Gravitational acceleration (9.81 m/s^2)
K	Taitel-Dukler parameter
T	Taitel-Dukler parameter
u_L	Superficial liquid velocity (m/s)
u_V	Superficial vapor velocity (m/s)
X	Baker parameter
X	Martinelli parameter
x	Vapor quality
Y	Baker parameter
a	Density of ambient air (kg/m^3)
L	Liquid density of refrigerant (kg/m^3)
V	Vapor density of refrigerant (kg/m^3)
wa	Density of ambient water (kg/m^3)
L	Liquid dynamic viscosity of refrigerant (Ns/m^2)
wa	Dynamic viscosity of ambient water (Ns/m^2)
'	Modified Baker parameter
	Baker parameter
L	Surface tension of refrigerant (N/m)
wa	Surface tension of ambient water (N/m)

REFERENCES

Collier, J.G. and Thome, J.R., 1993. Convective Boiling and Condensation, 3rd Edition, Oxford University Press, Oxford (expected publication date of new 3rd Edition is December, 1993).

Du Pont (1993). Thermodynamic Properties of SUVA HP80 Refrigerant, Report T-HP80-SI, Wilmington, Deleware.

Gungor, K.E. and Winterton, R.H.S., 1986. A General Correlation for Flow Boiling in Tubes and Annuli, Int. J. Heat Mass Transfer, Vol. 29, pp. 351-358.

Gungor, K.E. and Winterton, R.H.S., 1987. Simplified General Correlation for Saturated Flow Boiling and Comparisons of Correlations with Data, Chem. Eng. Res. Des., Vol.65, pp. 148-156.

Hashizume, K., 1983. Flow Pattern and Void Fraction of Refrigerant Two-Phase Flow in a Horizontal Pipe, Bulletin of JSME, Vol. 26, No. 219, pp. 1597-1602.

Kandlikar, S.G., 1990. A General Correlation of Saturated Two-Phase Flow Boiling Heat Transfer Inside Horizontal and Vertical Tubes, J. Heat Transfer, Vol. 112, pp. 219-228.

Kattan, N., Thome, J.R. and Favrat, D., 1992. Convective Boiling and Two-Phase Flow Patterns in an Annulus, Proc. 10th National Heat Transfer Congress (Italian), UIT, Genoa, June 25-27, pp. 309-320.

Klimenko, V.V. and Fyodorov, M., 1990. Prediction of Heat Transfer for Two-Phase Forced Flow in Channels of Different Orientation, Proc. 9th International Heat Transfer Conf., Vol. 5, pp. 65-70.

REFPROP (1992). Thermodynamic Properties of Refrigerants and Refrigerant Mixtures, Version 3.04a, National Institute of Standards and Technology (NIST), Gaithersburg, MD 20899.

Shah, M.M., 1982. Chart Correlation for Saturated Boiling Heat Transfer: Equations and Further Study, ASHRAE Trans., Vol. 88, Part 1, pp. 185-196.

Steiner, D. and Taborek, J., 1992. Flow Boiling Heat Transfer in Vertical Tubes Correlated by an Asymptotic Model, Heat Transfer Engineering, Vol. 13, No. 2, pp. 43-69.

Taitel, Y. and Dukler, A.E., 1976. A Model for Predicting Flow Regime Transitions in Horizontal and Near Horizontal Gas-Liquid Flow, AIChE J., Vol. 22, No. 1, pp. 47-55.

Thome, J.R., 1993. Thermodynamic and Transport Properties of Refrigerant R134a, LENI Technical Report, Swiss Federal Institute of Technology, Lausanne, Switzerland (Jan. 12).